British Journal of Pharmacology (2006) 147, 476–485
www.nature.com/bjp

Interspecies pharmacokinetics and *in vitro* metabolism of SQ109

*,[1]Lee Jia, [2]Patricia E. Noker, [2]Lori Coward, [2]Gregory S. Gorman, [3]Marina Protopopova & [1]Joseph E. Tomaszewski

[1]Developmental Therapeutics Program, National Cancer Institute, NIH, 6130 Executive Blvd., Rm 8042, Rockville, MD 20852, U.S.A.; [2]Southern Research Institute, Birmingham, AL, U.S.A. and [3]Sequella Inc., Rockville, MD, U.S.A.

1 This study aimed at characterizing the interspecies absorption, distribution, metabolism and elimination (ADME) profile of *N*-geranyl-*N*′-(2-adamantyl)ethane-1,2-diamine (SQ109), a new diamine-based antitubercular drug.

2 Single doses of SQ109 were administered (intravenously (i.v.) and *per os* (p.o.)) to rodents and dogs and blood samples were analyzed by liquid chromatography tandem mass spectrometry (LC/MS/MS). Based on i.v. equivalent body surface area dose, the terminal half-life ($t_{1/2}$) of SQ109 in dogs was longer than that in rodents, reflected by a larger volume of distribution (V_{ss}) and a higher clearance rate of SQ109 in dogs, compared to that in rodents. The oral bioavailability of SQ109 in dogs, rats and mice were 2.4–5, 12 and 3.8%, respectively.

3 After oral administration of [^{14}C]SQ109 to rats, the highest level of radioactivity was in the liver, followed by the lung, spleen and kidney. Tissue-to-blood ratios of [^{14}C]SQ109 were greater than 1. Fecal elimination of [^{14}C]SQ109 accounted for 22.2% of the total dose of [^{14}C]SQ109, while urinary excretion accounted for only 5.6%. The binding of [^{14}C]SQ109 (0.1–2.5 μg ml^{-1}) to plasma proteins varied from 6 to 23% depending on the species (human, mouse, rat and dog).

4 SQ109 was metabolized by rat, mouse, dog and human liver microsomes, resulting in 22.8, 48.4, 50.8 or 58.3%, respectively, of SQ109 remaining after a 10-min incubation at 37°C. The predominant metabolites in the human liver microsomes gave intense ion signals at 195, 347 and 363 m/z, suggesting the oxidation, epoxidation and *N*-dealkylation of SQ109. *P*450 reaction phenotyping using recombinant cDNA-expressed human CYPs in conjunction with specific CYP inhibitors indicated that CYP2D6 and CYP2C19 were the predominant CYPs involved in SQ109 metabolism.
British Journal of Pharmacology (2006) **147,** 476–485. doi:10.1038/sj.bjp.0706650;
published online 23 January 2006

Keywords: Antituberculosis; diamine; SQ109; ADME; pharmacokinetics

Abbreviations: ADME, absorption distribution metabolism elimination; CL, clearance rate; ESI, electrospray ionization; d.p.m., disintegrations per min; LC/MS/MS, liquid chromatography tandem mass spectrometry; V_{ss}, volume of distribution; $t_{1/2}$, terminal half-life

Introduction

Identification of a promising new compound for the treatment of tuberculosis is exciting, and its development is very challenging (Barry III *et al*., 2000). Current regimens require combined treatment of tuberculosis with multiple drugs, including isoniazid, rifampin, ethambutol and pyrazinamide for the full dosing period of 6 months (American Thoracic Society Documents, 2003). It is difficult to comply completely with this complex and prolonged regimen, and consequently, there is a substantial rate of treatment failure, even among patients with drug-sensitive disease. Thus, the availability of a more potent antibiotic that could clear infection more rapidly would be very valuable.

Many approaches to screening and identifying antibiotics start with a search for biochemical inhibitors of potential targets and then focus on those that inhibit microbial growth (Rubin, 2005). Lee *et al*. (2003) started with a diverse library of 63 238 ethambutol analogs with 1,2-diamine pharmacophore and tested their activity against *Mycobacterium tuberculosis* using high-throughput screening. The initial rationale was to identify diamine analogs with enhanced efficacy over ethambutol to improve the existing treatment of tuberculosis, and hopefully make therapeutic implementation easier and of shorter duration. After the lead optimization and screening, three analogs were found to have an enhanced antitubercular activity compared to ethambutol. Based on the results obtained from comparisons of effectiveness and high-throughput pharmacokinetic screening using cassette dosing combined with liquid chromatography tandem mass spectrometry (LC/MS/MS) (Jia *et al*., 2005a), we selected *N*-geranyl-*N*′-(2-adamantyl)ethane-1,2-diamine (SQ109, MW 330.2; see Figure 5 for SQ109 structure) as a lead compound for advanced drug testing. SQ109 exhibited both *in vitro* antimicrobial activity against *M. tuberculosis* strain H37Rv grown inside the host murine macrophage cells and *in vivo* antimicrobial activity on the mouse model inoculated with the H37Rv strain. Oral administration of SQ109 to mice for 28 consecutive days resulted in significant reductions in mycobacterial burden in both the lungs and spleen of the mice. Monitoring SQ109 levels in mouse vital tissues in the course of 28-day oral administration showed that the potential sites of action (e.g., lungs and spleen) contained SQ109 at

*Author for correspondence; E-mail: jiale@mail.nih.gov

concentrations that were at least 10 times higher than its minimal inhibitory concentration (1.56 μM). SQ109 displayed a large volume of distribution to various tissues. Despite its low oral bioavailability, the targeted tissue concentrations of SQ109 were at least 120-fold higher than that in the plasma (Jia *et al*., 2005b). Fingerprinting of SQ109 pharmacoproteomics indicates that treatment of *M. tuberculosis* H37Rv strain with SQ109 caused significant upregulation of secreted antigenic proteins ESAT-6-, CFP-10- and ATP-dependent DNA/RNA helicase, and downregulation of β-ketoacyl-acyl carrier protein synthase (Jia *et al*., 2005a).

The purpose of the present studies was to characterize systematically and comprehensively the preclinical profile of absorption, distribution, metabolism and elimination (ADME) for SQ109 in a number of species, including its pharmacokinetics, plasma protein binding; tissue distribution and urinary and fecal elimination in rats; as well as its *in vitro* metabolism, metabolism phenotyping and possible metabolic pathways.

Methods

Animals

Male CD2F1 mice (23–27 g), male Fischer rats (271–289 g) and beagle dogs (7.5–8.9 kg, two males and two females per dose group) were handled in accordance with the Guide for the Care and Use of Laboratory Animals (National Research Council, 1996), or the Principles of Laboratory Animal Care (http://history.nih.gov/laws).

Analytical method for determining SQ109 in biomatrices

The analytical method for determining SQ109 in various biomatrices was similar to that described previously (Jia *et al*., 2005b). Briefly, separation of SQ109 from biomatrices was achieved on a β-basic C_{18} analytical column preceded by a C_{18} guard column (Keystone Scientific, Bellefonte, PA, U.S.A.) at 25°C and a flow rate of 0.6 ml min^{-1}. SQ109 and terfenadine (internal standard) were eluted using a mobile phase composed of buffer A (5 mM CH_3COONH_4 with 0.1% trifluoroacetic acid, pH 6.8) and buffer B (methanol with 0.1% trifluoroacetic acid) according to the following gradient program: 50% buffer A and 50% buffer B were held for 0.5 min, and then buffer A was linearly decreased to 20% over 3 min and remained constant for 1 min while the analytes were eluted. The column was re-equilibrated to initial conditions *via* a step gradient for 3 min. A PE Sciex API 3000 triple quadrupole mass spectrometer equipped with a Turbo Ion spray source and operating at 450°C in the positive ion mode was used for the analysis of SQ109. The lower limit of quantitation of SQ109 in the plasma was determined to be 1.95 ng ml^{-1}.

Rat and dog pharmacokinetic studies with SQ109

Rats with an indwelling jugular vein catheter were used for the pharmacokinetic studies. Rats were given either a single intravenous (i.v.) bolus dose of 1.5 mg kg^{-1} (9 mg m^{-2}) or an oral dose of 13 mg kg^{-1} (78 mg m^{-2}) of SQ109 ($n=8$ per dose group); rats were divided into subgroups consisting of four rats per subgroup. Rat blood (0.7 ml) was withdrawn from the jugular vein catheter at alternating time points from individual rats in each subgroup. Blood samples were collected at 2, 5, 10, 15 and 30 min and 1, 3, 6, 10 and 24 h after a single i.v. administration, or 5, 15 and 30 min and 1, 2, 4, 6, 10 and 24 h after a single oral administration. Each blood sample was centrifuged to separate plasma, which was then stored at −70°C until analysis.

Beagle dogs were dosed by gavage at either 3.75 or 15 mg kg^{-1} (75 or 300 mg m^{-2}), or intravenously at either 0.45 or 4.5 mg kg^{-1} (9 and 90 mg m^{-2}). Dog blood (0.7 ml) was withdrawn from the jugular vein at 2, 5, 10, 20 and 30 min and 1, 2, 4, 8, 12, 18 and 24 h after a single i.v. administration, or 10, 20 and 30 min and 1, 2, 4, 8, 12, 18 and 24 h after a single oral administration.

Each blood sample was collected into a tube containing EDTA and centrifuged ($2000 \times g$, 10 min) to separate plasma and red blood cells. To each 200 μl of plasma sample, 10 μl of internal standard solution (10 μg ml^{-1}) was added. SQ109 was then separated and analyzed by the LC/MS/MS method according to the previously described procedures (Jia *et al*., 2005b). Peak area ratios of SQ109 to the internal standard were plotted against theoretical concentrations. Drug concentrations in the plasma samples were calculated from the standard calibration curves. Pharmacokinetic parameters were calculated using the computer program WinNonlin (Pharsight Co., Mountain View, CA, U.S.A.), and bioavailability was calculated as $(AUC_{p.o.}\, AUC_{i.v.}^{-1}) \times (dose_{i.v.}\, dose_{p.o.}^{-1}) \times 100\%$.

Tissue distribution and elimination of [^{14}C]SQ109 in rats

[^{14}C]SQ109 (5.8 mg ml^{-1}) was diluted 4.4-fold with 0.9% sterile saline to yield a formulation containing 1.3 mg ml^{-1} SQ109 (225 μCi ml^{-1}). Male Fischer rats (271–289 g) were individually housed in metabolism cages from which urine and feces were cumulatively collected to determine [^{14}C]SQ109 excretion rate. The rats were orally dosed by gavage with 13 mg kg^{-1} of [^{14}C]SQ109. Rats were killed at 0.5, 5, 10 and 24 h after dosing ($n=3$ per time point) in order to collect blood, tissues and organs for quantitative analysis. Tissues, intestinal tract contents and feces were homogenized in 10 volumes of water. Duplicate aliquots of whole blood, homogenates of tissues, intestinal contents and feces were digested with tissue solubilizer Soluene 350, and decolorized with 30% hydrogen peroxide to eliminate chemiluminescence. The samples were radioassayed after mixing with glacial acetic acid and the scintillation cocktail. Duplicate aliquots of urine and cage rinses were radioassayed after mixing with scintillation cocktail.

Pieces of carcasses were digested with 650 ml of 10 N sodium hydroxide, maintained at 37°C for 3 days, and then at room temperature until complete dissolution of the carcasses (~2 weeks). Quadruplicate aliquots of each dissolved carcass were diluted with water (1 : 20, v v^{-1}); portions of each diluted sample were radioassayed after the addition of an appropriate scintillator. After correction for volume by dilution and volume assayed, the radioactivity expressed as disintegrations per min (d.p.m.) of [^{14}C]SQ109 in each sample was determined.

Plasma protein binding

The percent binding of [^{14}C]SQ109 to mouse, rat, dog and human plasma proteins was determined by using ultracentrifugation (Barre *et al*., 1985; Boulton *et al*., 1998). Briefly,

spiking solutions of [^{14}C]SQ109 were prepared by diluting the stock [^{14}C]SQ109 (1 mCi of 5.9 mg^{-1} ml^{-1}) with absolute ethanol to yield spiking solutions containing 5, 25 or 125 μg ml^{-1} of [^{14}C]SQ109. For each species, a 10.8 ml aliquot of plasma was mixed with 0.22 ml of the appropriate spiking solution of [^{14}C]SQ109 to yield final SQ109 concentrations of 0.1, 0.5 or 2.5 μg ml^{-1}. The plasma mixtures were placed into individual polycarbonate ultracentrifuge tubes and centrifuged at 100,000 $\times$ g for 24 h at 4°C.

At the end of the centrifugation period, the upper chylomicron layer, middle aqueous layer and lower protein pellet were separated and the volume of each layer was determined. The protein pellets were dissolved in Soluene 350 tissue solubilizer. The radioactivity of duplicate portions of the chylomicron and aqueous layers as well as the solubilized protein layer was determined, and the total amount of radioactivity in each layer was calculated. The percentage of radioactivity in each layer was determined by comparing the amount of radioactivity in each layer with the sum of the total amount of radioactivity in all three postcentrifugation plasma samples. The percent of the total radioactivity in the aqueous layer was considered to represent the unbound fraction of SQ109, while the sum of the radioactivity in the chylomicron and lower (pellet) protein layers was considered to represent the bound fraction of the drug.

Radioactivity determination

The radioactivity of all samples was measured in the Tri-Carb 2100TR liquid scintillation analyzer. All counts were converted to absolute radioactivity (d.p.m.) by automatic chemiluminescence and quench correction. Samples having radioactivity (d.p.m.) less than or equal to twice background d.p.m. were considered to be below the limit of quantitation, and therefore the reading was considered zero d.p.m. for calculation purposes. SQ109 equivalents in biological samples were determined by dividing the sample d.p.m. by the specific activity of [^{14}C]SQ109 in d.p.m. per microgram, and expressed in microgram per gram of tissue. [^{14}C]SQ109 equivalents were also expressed as a percentage of [^{14}C]SQ109 amount in organs or tissues over the administered total [^{14}C]SQ109 amount per animal. The radioactivity in rat urine and feces was expressed as a percentage of the administered dose for each time interval and as a cumulative percentage.

Microsomal metabolism of SQ109

The microsomal assay was similar to that described previously (Jia *et al*., 2003). Briefly, SQ109 (10 μM) was incubated with mouse, rat, dog and human liver microsomes, respectively, in an NADPH-generating system containing 1.3 mM NADP, 3.3 mM glucose-6-phosphate, 0.4 U/ml glucose-6-phosphate dehydrogenase and 3.3 mM $MgCl_2$ in 100 mM potassium phosphate buffer (pH 7.4). Reaction mixtures were prepared in duplicate and were preincubated for 5 min at 37°C. The reactions were then initiated by the addition of microsomes (30 μl of a 20 mg ml^{-1} solution in 250 mM sucrose, yielding a final protein concentration of 0.5 mg ml^{-1}). The final volume of each reaction mixture was 1.2 ml. Negative control reactions were prepared by incubating mixtures that excluded either microsomes or SQ109 from the mixture. For negative control incubation where microsomes were excluded, they were added back to the reaction mixture after quenching with acetonitrile. Samples were removed at 0, 10, 20, 40 or 80 min and vortex-mixed with cold acetonitrile to stop the reaction. After centrifugation, a portion of each resulting supernatant was analyzed by mass spectrometry for unchanged SQ109.

Metabolism of SQ109 by cDNA-expressed recombinant human CYPs

SQ109 metabolism was also evaluated in microsomes prepared from insect cells transfected with cDNAs encoding for human CYP1A2, CYP2A6, CYP3A4, CYP2B6, CYP2C8, CYP2C9, CYP2C19 or CYP2D6. The recombinant enzymes and microsomes from untransfected insect cells were used in parallel as a control. SQ109 (10 μM) was preincubated in duplicate with the above-mentioned NADPH-generating system for 5 min at 37°C. The reactions were then initiated by the addition of the individual CYPs (final 100 pmol CYP ml^{-1}) or corresponding untransfected cells. Samples were mixed by inversion, removed at 0 and 30 min and mixed with ice-cold acetonitrile to stop the reactions. After centrifugation (14,000 $\times$ g for 20 min at 4°C), each extract was analyzed by using the mass spectrometry to monitor metabolite formation or SQ109 depletion. Electrospray ionization (ESI) full mass scans were performed to obtain the ion chromatograms of the expected metabolites according to predicted mass gains and losses as compared with the molecular mass of SQ109. The ESI as a gentle ionization technique is preferred in metabolite analysis, since ESI usually does not dissociate compounds extensively. The metabolite profiling was based on the detection of protonated, deprotonated or adduct ions, but not on the fragment ions (Kostiainen *et al*., 2003). Samples were assayed in both the negative and positive ion to ensure detection of all potential metabolite(s), and define the structure(s). Metabolite quantitation was based on percentages of peak areas of each metabolite as a function of incubation time compared to the total area of all chromatographic peaks.

Chemical inhibition studies

The following inhibitors, at the concentrations shown, were incubated with the corresponding CYP isoforms. These concentrations were based on literature information (Parkinson, 1996; Tucker *et al*., 2001; Bjornsson *et al*., 2003): furafylline (CYP1A2; 0.1, 1 and 10 μM), quinidine (CYP2D6; 0.5, 1 and 10 μM), ticlopidine (CYP2C19; 5, 20 and 100 μM) (Donahue *et al*., 1997; Tateishi *et al*., 1999; Ha-Duong *et al*., 2001) and troleandomycin (CYP3A; 0.5, 1 and 10 μM). All inhibitors were dissolved in methanol prior to addition to the incubation mixtures. Reaction mixtures containing human cDNA expressed CYP2D6 or CYP2C19 (100 pmol P450 ml^{-1} reaction mixture), the NADPH-generating system, selective CYP inhibitors and 100 mM potassium phosphate buffer (pH 7.4) were preincubated for 15 min at 37°C. Each reaction was then started by the addition of SQ109 (10 μM) with subsequent mixing of each sample by inversion. The samples were immediately removed and mixed with cold acetonitrile to stop reaction at 0 and 30 min of incubation. SQ109 and its metabolites were identified by the LC/MS/MS method. Peak areas formed were used for quantitative analyses. Control incubation mixtures included mixtures without inhibitors, and mixtures with untransfected insect cell microsomes used as

microsomal control, and mixtures that contained methanol instead of inhibitor (methanol control). Quantitative analyses were performed by comparing the peak areas of the inhibition reactions to their respective methanol controls. The total organic solvent content of the *in vitro* reaction mixtures was less than 2%.

Materials

[^{14}C]SQ109 was prepared in ethanol (1 mCi ml^{-1}) with specific activity and radiochemical purity (HPLC analysis) of 172 μCi mg^{-1} (57 mCi mmol^{-1}) and 99.6%, respectively. Tissue solubilizer Soluene 350 and Tri-Carb 2100TR liquid scintillation analyzer were purchased from Perkin-Elmer Life and Analytical Sciences (Boston, MA, U.S.A.). Scintillation cocktail (Safety SolveTM complete counting cocktail) was purchased from Research Products International Co. (Mount Prospect, IL, U.S.A.). All liver microsomes, human CYP isoforms and specific CYP isoform inhibitors were purchased from BD Gentest (Woburn, MA, U.S.A.). Organic solvents used in chromatographic separation of SQ109 were purchased from EM Science (Gibbstown, NJ, U.S.A.).

Statistical analysis

Data are expressed as the mean ± s.d. Statistical analysis was performed with Student's *t*-test for paired observation (two-tailed). A probability of 0.05 or less was considered significant.

Results

Pharmacokinetics of SQ109 in rats and dogs

SQ109 plasma concentration–time courses after single oral and i.v. administration to rats and dogs are illustrated in Figures 1 and 2, respectively. Pharmacokinetic parameters calculated from noncompartmental analysis of SQ109 concentrations in rat and dog plasma are presented in Tables 1 and 2, respectively. Interspecies pharmacokinetics are summarized in Table 3. The major pharmacokinetic parameters such as $t_{1/2}$, V_{ss}, clearance rate (CL) and oral bioavailability were compared in Table 3 among mice (Jia *et al*., 2005b) rats and dogs at the same dose based on equivalent body surface area (9 mg m^{-2}). The terminal $t_{1/2}$ of SQ109 in dogs (12–29 h; Table 2) was longer than in rats (7–8 h; Table 1), as reflected by the significantly larger volume of distribution of SQ109 in dogs, while the CL in dogs was higher than that in rats in comparison on body surface area dose. The i.v. C_{max} and AUC in dogs increased in proportion to the increase in doses, whereas the oral C_{max} and AUC were less proportional to the increase in doses probably because of the low oral bioavailability of SQ109 in dogs (2.4–5%; Table 2). The oral bioavailability of SQ109 in rats was determined to be 12%. Compared to the pharmacokinetic profiles of rats and dogs, male CD2F1 mice given the same dose of SQ109 scaled by body surface area (9 mg m^{-2}, i.v.; 75 mg m^{-2}, p.o.) showed a pharmacokinetic profile (Jia *et al*., 2005b) similar to rats, but different from dogs in terms of $t_{1/2}$, CL and V_{ss}, probably

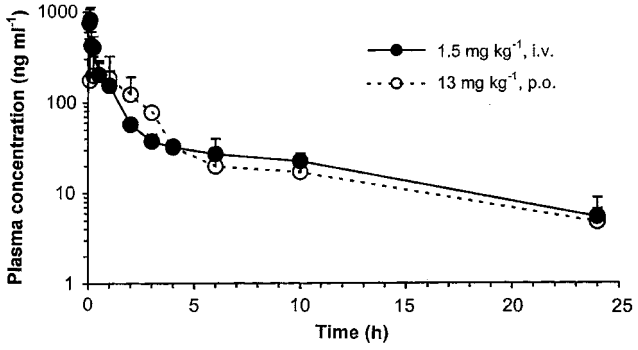

Figure 1 Plasma concentration–time courses of SQ109 after i.v. (1.5 mg kg^{-1}) and oral (13 mg kg^{-1}) administrations to rats. Each point represents the mean ± s.d. of eight rats.

Table 1 Pharmacokinetic parameters of SQ109 in rats ($n = 8$)[a]

Route	*i.v.*	*p.o.*
Dose		
(mg kg^{-1})	1.5	13
(mg m^{-2})	9	78
C_{max} (ng ml^{-1})	—	644
T_{max} (h)	—	0.5
$t_{1/2}$ (h)	7.4	8.2
$AUC_{0-\infty}$ (ng h^{-1} ml^{-1})	953	992
CL (ml kg^{-1} h^{-1})	1575	—
V_{ss} (ml kg^{-1})	9964	—
Bioavailability (%)	—	12

[a]Noncompartmental analysis.

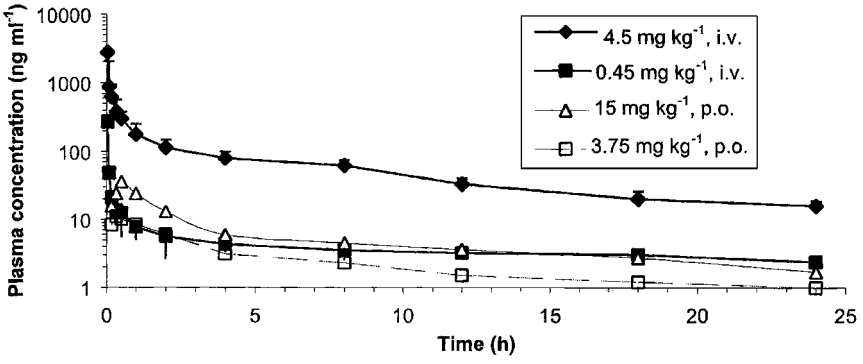

Figure 2 Plasma concentration–time courses of SQ109 after i.v. (0.45 or 4.5 mg kg^{-1}) and oral (3.75 or 15 mg kg^{-1}) administration to beagle dogs. Each point represents the mean ± s.d. ($n = 4$).

Table 2 Noncompartmental analysis of pharmacokinetic parameters of SQ109 in beagle dogs (mean ± s.d., $n = 4$)

Routes	*i.v.*	*i.v.*	*p.o.*	*p.o.*
Dose				
($mg\,kg^{-1}$)	0.45	4.5	3.75	15
($mg\,m^{-2}$)	9	90	75	300
C_{max} ($ng\,ml^{-1}$)	271 ± 109	2762 ± 1180**	11.7 ± 1.7	37.1 ± 6.5**
T_{max} (h)	—	—	0.59 ± 0.16	0.51 ± 0.09
$t_{1/2}$ (h)	29.3 ± 8.1	12.4 ± 3.01**	19.6 ± 4.8	11.6 ± 1.5*
$AUC_{0-\infty}$ ($ng\,h^{-1}\,ml^{-1}$)	223 ± 31	1942 ± 315**	86.5 ± 16.0	158 ± 34**
CL ($ml\,kg^{-1}\,h^{-1}$)	2138 ± 295	2471 ± 319	—	—
V_{ss} ($ml\,kg^{-1}$)	75,200 ± 19,100	29,200 ± 6940*	—	—
Bioavailability (%)	—	—	5.0 ± 2.4	2.4 ± 0.7

*$P < 0.05$, **$P < 0.01$, compared with the values obtained from lower doses of the same administration route.

Table 3 Comparison of major pharmacokinetic parameters of SQ109 administered i.v. to mice, rats and dogs at the same dose ($mg\,m^{-2}$)[a]

Species	*Dose* ($mg\,m^{-2}$)	$t_{1/2}$ (h)	*CL* ($ml\,m^{-2}\,h^{-1}$)	V_{ss} ($ml\,m^{-2}$)	*Oral bioavailability* (%)[b]
Mouse[c]	9	5.3	11,364	35,400	3.8
Rat	9	7.4	9450	59,700	12
Dog	9	29.3	42,760	1,504,000	5

[a]The conversion factors used for changing a dose expressed in terms of $mg\,kg^{-1}$ to an equivalent surface area dose $mg\,m^{-1}$ are 3 (mouse), 6 (rat) and 20 (dog), respectively, referring to the FDA Guidance http://www.fda.gov/cber/gdlns/dose.pdf.
[b]Note, the oral bioavailability was determined based on oral administration of $75\,mg\,m^{-2}$ of SQ109 to the animals.
[c]The mouse data were obtained from our previous studies (Jia *et al*., 2005b).

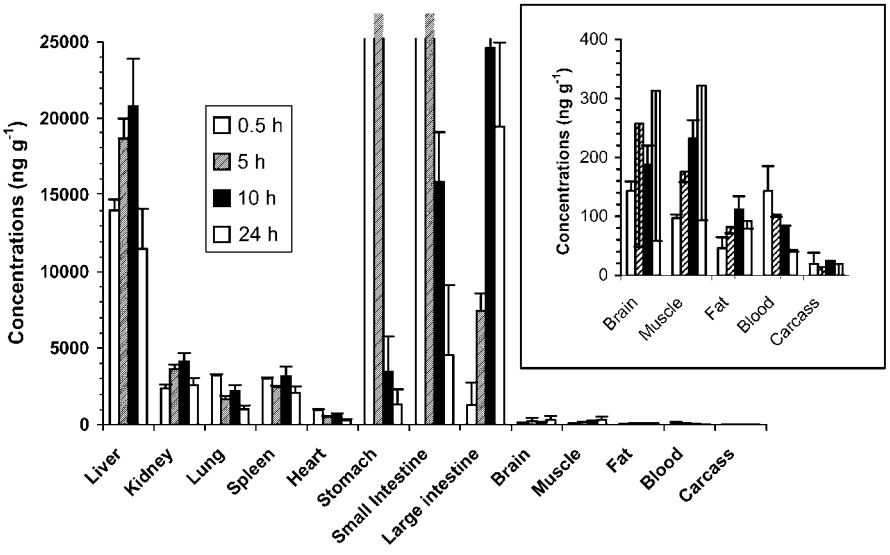

Figure 3 [^{14}C]SQ109 equivalent concentrations ($ng\,g^{-1}$) in tissue (mean ± s.d., $n = 3$) after oral administration to rats ($13\,mg\,kg^{-1}$). The inset magnifies the scale of [^{14}C]SQ109 concentrations in tissues and organs that contain low levels of [^{14}C]SQ109. The actual concentrations (off the scale) of [^{14}C]SQ109 in the stomach and small intestine were 450,000 ± 179,000 and 70,500 ± 9000 $ng\,g^{-1}$, respectively, at 0.5 h, and 173,000 ± 62,000 and 66,600 ± 19,800 $ng\,g^{-1}$ at 5 h after the single oral administration.

because rodents share the same allometric exponent that is different from that of dogs. Although no acute toxicity and pathological effects were identified, emesis was observed in dogs 10 min after oral administration of the high dose of SQ109 ($750\,mg\,m^{-2}$); the emesis was dose related, and most likely a consequence of gastric irritation.

[^{14}C]SQ109 tissue distribution and elimination in rats

Figure 3 shows [^{14}C]SQ109 levels in various tissues of rats at 0.5, 5, 10 and 24 h after oral administration of the radioactive compound ($13\,mg\,kg^{-1}$). In general, excluding the concentrations of [^{14}C]SQ109 in gastrointestinal tract, the highest concentrations of radioactivity were found in the liver, and the lowest in the fat. At each time point, [^{14}C]SQ109 concentrations in the lung, spleen and kidney were similar to each other, and ranked as the tissues containing the second highest concentrations of [^{14}C]SQ109. At 0.5 h after oral administration, [^{14}C]SQ109 concentrations in the brain and whole blood were the same ($143\,ng\,g^{-1}$). At 5, 10 and 24 h time points, [^{14}C]SQ109 concentrations in the brain were 257, 187 and $313\,ng\,g^{-1}$, respectively, which were higher than those in

whole blood at the same time points (103, 82 and 43 ng ml^{-1}), suggesting that the compound crosses the blood–brain barrier. Tissue-to-blood level ratios were generally greater than 1, indicating that the compound has the capability to move across blood vascular wall, distribute and reside in various tissues. The total equivalent concentrations of [^{14}C]SQ109 in the stomach, small intestine and large intestine at 0.5 h after the oral administration were 331±71, 312±67 and 3.4±1.9 μg g^{-1}, respectively. At 24 h, the concentrations declined to 2.1±3.3, 31±12 and 279±127 μg g^{-1}, respectively, kinetically reflecting the gastrointestinal transit time and absorption time of [^{14}C]SQ109.

By 24 h after oral administration, [^{14}C]SQ109 was eliminated mainly *via* the feces, which accounted for 22.2% of the total dose, while urinary excretion accounted for only 5.6% of the total dose (Table 4). The excretion rate (μg h^{-1}) of [^{14}C]SQ109 *via* urine was faster than that *via* feces during the first 10 h period. Thereafter, [^{14}C]SQ109 excretion rate *via* feces became predominating factor.

SQ109 plasma protein binding

The results of the protein binding determinations for mouse, rat, dog and human plasma are presented in Table 5.

In vitro *metabolism of SQ109 in liver microsomes*

The mass spectrometric analyses of SQ109 from the *in vitro* metabolism samples suggest that the parent compound SQ109 is rapidly metabolized when incubated with mouse, rat, dog or human liver microsomes (Figure 4). After incubation at 37°C for 10 min, the remaining SQ109 accounted for 22.8, 48.4, 50.8 and 58.3% of the total SQ109 initially added to rat, mouse, dog and human liver microsomal reaction mixtures, respectively. The fastest rate of metabolism of SQ109 occurred in rat liver microsomes, where essentially all of the added SQ109 was metabolized within 20 min. The slowest rate of metabolism occurred in human liver microsomes, where 8.1% of the added SQ109 remained after 40 min incubation at 37°C. In contrast, the percentage of SQ109 remaining in the negative control sample after 80-min incubation was 96.5, 100.0, 116.5 and 111.5 for human, rat, mouse and dog liver microsomes, respectively, as compared to the 0 min sample. The control result suggests involvement of liver microsomes in SQ109 metabolism.

Liver microsomes converted SQ109 (*m*/*z* 331.5) to four predominant metabolites with mass to charge ratios (*m*/*z*) at 195, 347, 361 and 363. Proposed metabolite identification using mass spectrometry suggests that *m*/*z* 361 named M1 symbolize an *N*-nitrosylation product of SQ109. The *m*/*z* 347 designated as M2 represents two metabolites (M2-1 and M2-2) with a single oxygen added to SQ109 at different locations, for example, the side chain and the adamantine ring. The *m*/*z* 195 represents a single metabolite obtained *via* an *N*-dealkylation reaction of an unstable intermediate and is designated M3. The *m*/*z* 363 (named as M4) is consistent in mass with two degrees of oxidation, that is, ring oxidation combined with *N*-hydroxylation (M4-1) or with epoxidation (M4-2) (Figure 5).

Metabolism by cDNA recombinant human CYPs

For the 30-min reaction mixtures containing CYP2A6, CYP2C8 or CYP2C9, no significant metabolite peaks were observed at the monitored masses. In addition, only negligible amounts of SQ109 metabolite at *m*/*z* 347 were found in incubations using individual recombinant CYP1A2, CYP3A4 or CYP2B6.

Extensive metabolism of SQ109 was observed in microsomes from insect cell lines transfected with cDNA from human CYP2D6 and CYP2C19. CYP2C19 showed the capacity to catalyze metabolism of SQ109 to produce metabolites of M1, M2, M3 and M4, while CYP2D6 primarily catalyzed SQ109 to form M1 and M4. Of great interest was the possible formation of *N*-(2-adamantyl)ethylene-1,2-diamine (M3, *m*/*z* 195) catalyzed by CYP2C19. M3 might contain the adamantane ring after cleavage of the N–C bond of SQ109 (Figure 5). Based on the degradation rate of SQ109 estimated by chromatographic peak areas over time, CYP2D6 was found to play the major

Table 4 Cumulative excretion (% of dose) and excretion rate of [^{14}C]SQ109 following a single oral dose of [^{14}C]SQ109 (13 mg kg^{-1}) to rats

Period after dosing (h)	*Excretion (% of dose)*		*Excretion rate* (μg h^{-1})	
	Urine	*Faeces*	*Urine*	*Faeces*
0–5	1.15±0.34	0.02±0.04	8.44±2.52	0.16±0.30
5–10	1.43±0.26	0.04±0.04	10.46±1.92	0.30±0.36
10–24	2.35±0.36	12.71±3.08	6.15±0.94	33.29±8.07
24–48	1.17±0.16	7.83±0.49	1.79±0.25	11.96±0.75
Total (0–48 h)	5.66±0.87	22.2±3.33	—	—

Excretion values are the mean±s.d. ($n=3$).

Table 5 Binding of [^{14}C]SQ109 at different concentrations to plasma protein

SQ109 (μg ml^{-1})	*% SQ109 bound to plasma protein from*			
	Mouse	*Rat*	*Dog*	*Human*
0.1	6.2, 7.8	8.4, 10.3	10, 11.4	14.3, 16.1
0.5	5.8, 8.4	8.1, 9.1	9.5, 11.7	16.3, 18.5
2.5	8.4, 8.5	8.4, 11.8	10.3, 12.1	17.8, 23.8

Data were obtained from two tests for each species.

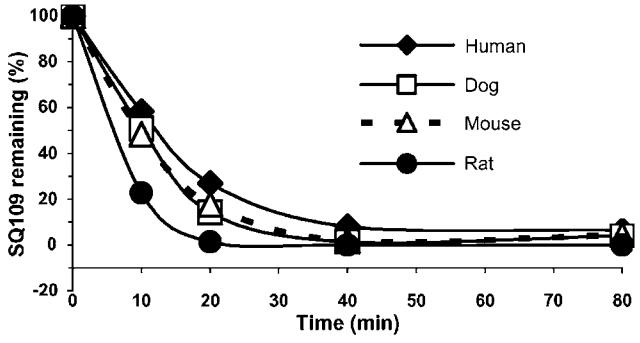

Figure 4 Metabolic rate of SQ109 (10 μM) incubated with liver microsomes from various species, at 37°C.

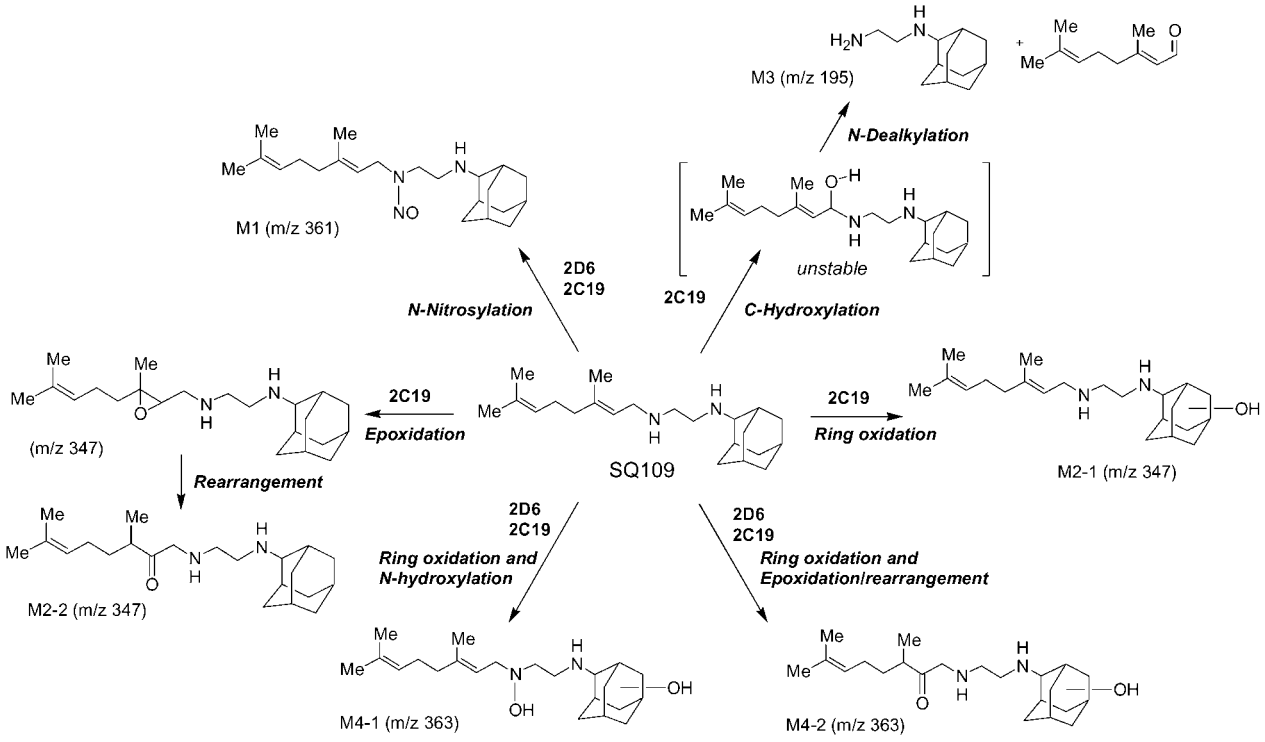

Figure 5 A schematic diagram depicting the proposed *in vitro* metabolic pathways of SQ109 and metabolites formed as a consequence of epoxidation, oxidation, dealkylation and nitrosylation in liver microsomes. See Discussion for details.

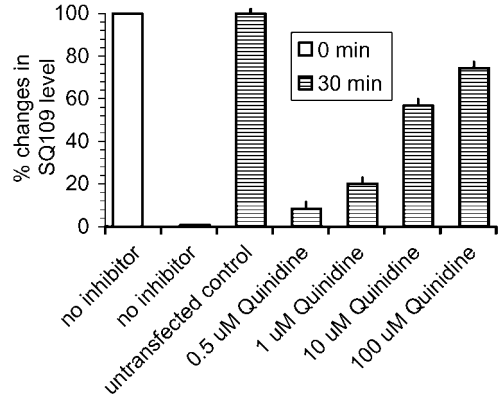

Figure 6 Dose-dependent inhibition by the CYP2D6 inhibitor, quinidine, of SQ109 metabolism induced by human CYP2D6. Note that in the absence of the inhibitor, SQ109 was almost completely metabolized within 30 min.

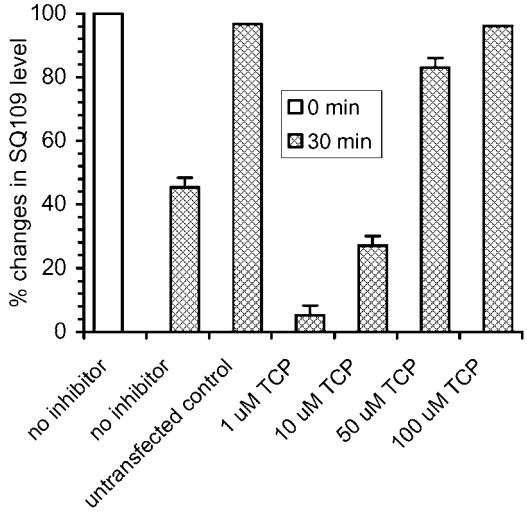

Figure 7 Dose-dependent inhibition by the CYP2C19 inhibitor, ticlopidine (TCP), of SQ109 metabolism induced by human CYP2C19. Note that in the absence of the inhibitor, SQ109 was partially metabolized within 30 min.

role in SQ109 metabolism at approximately 800 pmol·min^{-1} mg protein concentration^{-1}. No metabolites of SQ109 were found in the control reaction mixture containing nontransfected cells, and in the reaction mixtures containing CYP isomers, except CYP2D6 and CYP2C19.

Effects of selective P*450 inhibitors*

When quinidine and ticlopidine were coincubated with 10 μM SQ109 in the presence of CYP2D6 or CYP2C19 for 30 min, the two specific inhibitors reversed CYP2D6- and CYP2C19-induced metabolism of SQ109 in a dose-dependent manner (Figures 6 and 7). For example, only 0.8% of SQ109 remained after a 30-min incubation with CYP2D6 in the absence of the inhibitor quinidine, whereas addition of quinidine (100 μM) prevented the CYP2D6-induced metabolism and 74% of the SQ109 survived unchanged after a 30-min incubation (Figure 6). High concentrations of quinidine also decreased M1 and M4 formation. There was 45% of SQ109 remaining after a 30-min incubation with CYP2C19 alone but, in the

presence of 100 μM ticlopidine, almost all the SQ109 (96%) was unchanged over the same period of incubation (Figure 7). High concentrations of ticlopidine completely inhibited the formation of M1 and M4, and partially inhibited the formation of M2 and M3.

Discussion

SQ109 is lipophilic and has low aqueous solubility. Its absorption time in the tested animal species should be comparable due to the similar nature of the biomembrane of intestinal epithelial cells across species and the absorptive process (simple diffusion) that is basically an interaction between a specific drug and the biomembrane (Lin, 1995; Martinez *et al*., 2002). This is supported by the results of the present studies, which show that the T_{max} of SQ109 ($\sim$0.5 h) was similar among mice, rats and dogs (Tables 1 and 2).

SQ109 possesses a large V_{ss} as do the other ethambutol analogs in mice (Jia *et al*., 2005b, c). The same observation was made in rats and dogs in the present studies. Although methods for the prediction of V_{ss} based on experimentally determined physicochemical parameters can predict the V_{ss} close to the actual value, it must be kept in mind that drug- or plasma-based models refer to the process of penetration into hypothetical homogeneous compartments as 'tissue penetration'. This concept is misleading, as it does not take into account the uniqueness of separate heterogeneous organ systems (Muller *et al*., 2004). Therefore, it rarely corresponds to a real volume, such as plasma volume, extracellular water or total body water. Drug distribution may be to any one or a combination of the tissues and fluids of the body. Furthermore, binding to tissue components may be so great that the V_{ss} is many times the total body size (Rowland & Tozer, 1995). Most importantly, it must be considered that the actual target space for anti-infective agents is the interstitial space fluid (Ryan, 1993).

Many drugs are subject to a 'first-pass effect' when absorbed from the gastrointestinal tract into the systemic circulation. The organs responsible for this effect (i.e., intestine, liver and lung) are serially arranged and can potentially reduce the extent of bioavailability. The contribution of each organ has been assessed indirectly by comparison of AUC values obtained by different routes of administration (Pang & Gillette, 1978). Based on SQ109 tissue concentration–time data (Figure 3), one may conclude that SQ109 readily permeates the biomembrane of intestinal epithelial cells because of the drug's relatively fast T_{max} ($\sim$0.5 h). The tissue concentration–time data also suggest that the liver plays a significant role in eliminating and metabolizing SQ109. This finding is based on the data that show that (1) liver contained the highest concentration of [^{14}C]SQ109 (excluding the gastrointestinal concentrations of [^{14}C]SQ109); (2) [^{14}C]SQ109 in the liver was at least 200-fold higher than that in whole blood; and (3) direct measurement of SQ109 *per se* by using the LC/MS/MS method showed that SQ109 concentration in the liver was significantly lower than those in the lung, spleen, kidney and heart (Jia *et al*., 2005b). However, radioactive measurement indicated that the liver contains the highest amount of radioactivity. This discrepancy can be explained on the basis that the LC/MS/MS method was developed to be highly specific for the parent molecule of the drug only and did not detect any of the compound's metabolites. The radioactivity measurement detects all ^{14}C-containing components, which would include the parent compound and any corresponding metabolites of SQ109. These data suggest that SQ109 does undergo a first-pass metabolic step in the liver before it reaches the systemic circulation.

Several factors may affect the CL of a certain drug, including plasma protein binding, metabolism and hepatic blood flow. For a drug with high CL, hepatic blood flow limits the drug's CL (Boxenbaum, 1980). This rule may explain the species difference in CL of SQ109. Although there were slight interspecies differences in the metabolism of SQ109 by liver microsomes (Figure 4), the CL of SQ109 in dogs was four times higher than in mice and rats, probably because dogs have a high hepatic blood flow (Davies & Morris, 1993). Kinetically, drug distribution is often defined as the ratio of amount of drug in the body to the plasma or blood concentration. SQ109 has relatively low binding to plasma proteins (Table 5), but high binding to tissue proteins (Jia *et al*., 2005b) and high permeability across biomembranes. Therefore, its volume of distribution across species is extremely high (Table 3). A drug's half-life is proportional to its volume of distribution, but inversely proportional to its clearance. The theory is supported by the results of the present studies that indicate a longer $t_{1/2}$ of SQ109 in dogs than in mice and rats (Table 3).

In the present studies, we used the ultracentrifugation technique to determine plasma protein binding, which avoids the nonspecific membrane binding in contrast to other plasma protein binding techniques (Barre *et al*., 1985). To determine the binding capacity and affinity of plasma protein to a drug, it is suggested that at least three concentrations of the drug (e.g., 0.1, 0.5 and 2.5 μg ml^{-1}) be applied and tested (Kariv *et al*., 2001; Jia *et al*., 2003) to clarify concentration-related changes in the extent of binding. As shown in Table 5, increases in total [^{14}C]SQ109 by five- and 25-fold resulted in only a slight increase in bound fraction of [^{14}C]SQ109. This result implies that the binding seems to be of low affinity and high capacity because the fraction of bound SQ109 is relatively constant over a 25-fold concentration range and independent of drug concentration.

Because of the first-pass effect, the oral bioavailability of SQ109 across animal species tested was relatively low (4–12%; Table 3), and was likely to be related to a high hepatic clearance of SQ109. Using liver microsomes from various species and CYP reaction phenotyping, we found that SQ109 was rapidly metabolized when incubated with liver microsomes (Figure 4), although the metabolism rate varied from species to species. The liver microsome-induced metabolism of SQ109 was observed again when SQ109 was incubated in individual CYP2D6 or CYP2C19 isozymes. Furthermore, selective inhibitors of CYP2D6 and CYP2C19 prevented the metabolism in a dose-dependent manner (Figures 6 and 7). Therefore, both CYP2D6 and CYP2C19 can be singled out as primary CYPs that catalyze SQ109 metabolism. CYP2D6 and CYP2C are involved in biotransformation of about 25 and 15% of all drugs (Parkinson, 1996; Schlichting *et al*., 2000; Tucker *et al*., 2001), respectively. Although low oral bioavailability of many drugs can be attributed to the extensive metabolism by CYP3A4, the present studies demonstrated little effect of CYP3A4 on SQ109 metabolism.

Based on the *P*450 reaction phenotyping study, we proposed the *in vitro* metabolic pathway of SQ109 shown in Figure 5.

N-nitroso-SQ109 (M1) could be formed *via* CYP2D6- and CYP2C19-catalyzed metabolism. Out of two amino groups in the molecule, the most vulnerable site of SQ109 known to be prone to electrophilic attack from −NO may be the second, the geranyl-substituted, amino group in the molecule. Biological nitrosation remains an issue that engenders controversy about biological reactivity and functions of nitrosation (Williams, 1988; Jia *et al*., 1996). Possible metabolism of SQ109 may also include addition of a single oxygen to SQ109, resulting in the formation of metabolite M2 with *m*/*z* 347. One of the metabolites (M2-1, *m*/*z* 347) is likely to be produced by oxidation of the adamantane ring, similar to the metabolism of a marketed adamantane-containing antiviral drug rimantadine. Another single oxygenated SQ109 metabolite (M2-2, *m*/*z* 347) may form through epoxidation of the *N*-allyl double bond in the geranyl moiety, leading to the corresponding epoxide that may further undergo thermal rearrangement resulting in the ketodiamine SQ109 (M2-2). *N*-(2-adamantyl)ethylene-1,2-diamine (M3, *m*/*z* 195) may be formed by fragmentation of the parent compound *via* hydroxylation of an activated carbon atom in the geranyl fragment followed by *N*-dealkylation of the unstable intermediate. The formation of M3 was demonstrated by a single mass chromatographic peak (not shown). There are several pathways to explain formation of M4 that may appear as different structures with the same *m*/*z* 363 because of the locations of the two oxygen atoms added to SQ109. It is highly likely that consequent oxidation reactions take place, such as ring oxidation and *N*-hydroxylation (M4-1, *m*/*z* 363) and/or ring oxidation and epoxidation (M4-2, *m*/*z* 363) processes that lead to the formation of corresponding hydroxy metabolites.

In the metabolic events occurring to SQ109 such as C-oxidation and *N*-hydroxylation (Figure 5), oxygen from the ferric state $(FeO)^{3+}$ of CYP450 could be incorporated into SQ109, which otherwise remains intact. In the case of *N*-dealkylation, oxygenation of SQ109 may be followed by a thermal rearrangement, leading to cleavage of an *N*-amantadine structure (M3) from the remaining aliphatic structure with incorporation of oxygen from the $(FeO)^{3+}$ complex into the aliphatic structure. Nonetheless, the reality of the metabolic pathway and significance of the *in vivo* effects of the produced end metabolites need to be further investigated and validated using authentic metabolites.

In conclusion, the present study systematically showed interspecies similarities and differences in ADME profile of SQ109, and its large V_{ss} and relatively low oral bioavailability. Oral [^{14}C]SQ109 produced the highest level of radioactivity in liver. This may represent a significant first-pass effect on SQ109, as evidenced by rapid liver microsomal metabolism of SQ109, primarily catalyzed by CYP2D6 and CYP2C19. Fecal and urinary elimination accounted for 22.2 and 5.6% of the total dose of [^{14}C]SQ109, respectively. None of these and our previous findings guarantee that SQ109 will be a successful antibiotic. Like any drug, it could turn out to be toxic during long-term use. Nevertheless, this is clearly the most promising new antituberculosis agent that has passed through many preclinical tests (Lee *et al*., 2003; Jia *et al*., 2005a–c).

This study was supported by the Inter-Institute Program of National Institutes of Health, and funded by NO1-CM-07110 and NO1-CM-52203 of the National Cancer Institute.

References

AMERICAN THORACIC SOCIETY DOCUMENTS. (2003). American Thoracic Society/Centers for Disease Control and Prevention/ Infectious Diseases Society of America: Treatment of Tuberculosis. *Am. J. Respir. Crit. Care Med.,* **167,** 603–662.

BARRE, J., CHAMOUARD, J.M., HOUIN, G. & TILLEMENT, J.P. (1985). Equilibrium dialysis, ultrafiltration, and ultracentrifugation compared for determining the plasma-protein-binding characteristics of valproic acid. *Clin. Chem.,* **31,** 60–64.

BARRY III, C.E., SLAYDEN, R.A., SAMPSON, A.E. & LEE, R.E. (2000). Use of genomics and combinatorial chemistry in the development of new antimycobacterial drugs. *Biochem. Pharmacol.,* **59,** 221–231.

BJORNSSON, T.D., CALLAGHAN, J.T., EINOLF, H.J., FISCHER, V., GAN, L., GRIMM, S., KAO, J., KING, S.P., MIWA, G., NI, L., KUWAR, G., MCLEOD, J., OBACH, R.S., ROBERTS, S., ROE, A., SHAH, A., SNIKERIS, F., SULLIVAN, J.T., TWEEDIE, D., VEGA, J.M., WALSH, J. & WRIGHTON, S.A. (2003). The conduct of *in vitro* and *in vivo* drug–drug interaction studies: a pharmaceutical research and manufacturers of America (PhRMA) perspective. *Drug Metab. Dispos.,* **31,** 815–832.

BOULTON, D.W., WALLE, U.K. & WALLE, T. (1998). Extensive binding of the bioflavonoid quercetin to human plasma proteins. *J. Pharm. Pharmacol.,* **50,** 243–250.

BOXENBAUM, H. (1980). Interspecies variation in liver weight, hepatic blood flow and antipyrine intrinsic clearance in extrapolation of data to benzodiazepines and phenytoin. *J. Pharmacokinet. Biopharmacol.,* **8,** 165–176.

DAVIES, B. & MORRIS, T. (1993). Physiological parameters in laboratory animals and humans. *Pharm. Res.,* **10,** 1093–1095.

DONAHUE, S.R., FLOCKHART, D.A., ABERNETHY, D.R. & KO, J. (1997). Ticlopidine inhibition of phenytoin metabolism mediated by potent inhibition of CYP2C19 *Clin. Pharmacol. Ther.,* **62,** 572–577.

HA-DUONG, N.T., DIJOLS, S., MACHEREY, A.C., DANSETTE, P.M. & MANSUY, D. (2001). Inhibition by ticlopidine and its derivatives of human liver cytochrome *p*450. Mechanism-based inactivation of CYP 2C19 by ticlopidine. *Adv. Exp. Med. Biol.,* **500,** 145–148.

JIA, L., BONAVENTURA, C., BONAVENTURA, J. & STAMLER, J.S. (1996). *S*-nitrosohaemoglobin: a dynamic activity of blood involved in vascular control. *Nature,* **380,** 221–226.

JIA, L., COWARD, L., GORMAN, S.G., NOKER, P. & TOMASZEWSKI, E.J. (2005a). Pharmacoproteomic effects of isoniazid, ethambutol, and *N*-geranyl-*N*′-(2-adamantyl)ethane-1,2-diamine (SQ109) on *Mycobacterium tuberculosis* H37Rv. *J. Pharmacol. Exp. Ther.,* **315,** 905–911.

JIA, L., TOMASZEWSKI, J., HANRAHAN, C., COWARD, L., NOKER, P., GORMAN, G., NIKONENKO, B. & PROTOPOPOVA, M. (2005b). Pharmacodynamics and pharmacokinetics of SQ109, a new diamine-based antitubercular drug. *Br. J. Pharmacol.,* **144,** 80–87.

JIA, L., TOMASZEWSKI, J.E., NOKER, P.E., GORMAN, G.S., GLAZE, E. & PROTOPOPOVA, M. (2005c). Simultaneous estimation of pharmacokinetic properties in mice of three anti-tubercular ethambutol analogues obtained from combinatorial lead optimization. *J. Pharm. Biomed. Anal.,* **37,** 793–799.

JIA, L., WONG, H., WANG, Y., GARZA, M. & WEITMAN, S.D. (2003). Carbendazim: disposition, cellular permeability, metabolite identification and pharmacokinetic comparison with its nanoparticle. *J. Pharm. Sci.,* **92,** 161–172.

KARIV, I., CAO, H. & OLDENBURG, K.R. (2001). Development of a high throughput equilibrium dialysis method. *J. Pharm. Sci.,* **90,** 580–587.

KOSTIAINEN, R., KOTIAHO, T., KUURANNE, T. & AURIOLA, S. (2003). Liquid chromatography/ atmospheric pressure ionization–mass spectrometry in drug metabolism studies. *J. Mass Spectrom.,* **38,** 357–372.

LEE, R., PROTOPOPOVA, M., CROOKS, E., SLAYDEN, R., TERROT, M. & BARRY, C. (2003). Combinatorial lead optimization of [1,2]-diamines based on ethambutol as potential anti-tuberculosis preclinical candidates. *J. Combin. Chem.,* **5,** 172–187.

LIN, J.H. (1995). Species similarities and differences in pharmacokinetics. *Drug. Metab. Dispos.,* **23,** 1008–1021.

MARTINEZ, M., AMIDON, G., CLARKE, L., JONES, W.W., MITRA, A. & RIVIERE, J. (2002). Applying the biopharmaceutics classification system to veterinary pharmaceutical products. Part II. Physiological considerations. *Adv. Drug Deliv. Rev.,* **54,** 825–850.

MULLER, M., PENA, A.D. & DERENDORF, H. (2004). Issues in pharmacokinetics and pharmacodynamics of anti-infective agents: distribution in tissue. *Antimicrob. Agents Chemother.,* **48,** 1441–1453.

NATIONAL RESEARCH COUNCIL. (1996). *Guide for the Care and Use of Laboratory Animals.* Washington, DC: National Academy Press.

PANG, K.S. & GILLETTE, J.R. (1978). Theoretical relationships between area under the curve and route of administration of drugs and their precursors for evaluating sites and pathways of metabolism. *J. Pharm. Sci.,* **67,** 703–704.

PARKINSON, A. (1996). Biotransformation of xenobiotics. In: *Casarett & Doull's Toxicology: The Basic Science of Poisons*. ed. Klaassen, C. pp. 113–186. New York: McGraw-Hill.

ROWLAND, M. & TOZER, T.N. (1995). *Clinical Pharmacokinetics Concepts and Applications,* pp. 20–21. Media: Lippincott Williams & Wilkins.

RUBIN, E.J. (2005). Toward a new therapy for tuberculosis. *N. Engl. J. Med.,* **352,** 933–934.

RYAN, D.M. (1993). Pharmacokinetics of antibiotics in natural and experimental superficial compartments in animals and humans. *J. Antimicrob. Chemother.,* **31** (Suppl D), 1–6.

SCHLICHTING, I., BERENDZEN, J., CHU, K., STOCK, A.M., MAVES, S.A., BENSON, D.E., SWEET, R.M., RINGE, D., PETSKO, G.A. & SLIGAR, S.G. (2000). The catalytic pathway of cytochrome *P*450cam at atomic resolution. *Science,* **287,** 1615–1622.

TATEISHI, T., KUMAI, T., WATANABE, M., NAKURA, H., TANAKA, M. & KOBAYASHI, S. (1999). Ticlopidine decreases the *in vivo* activity of CYP2C19 as measured by omeprazole metabolism. *Br. J. Clin. Pharmacol.,* **47,** 454–457.

TUCKER, G.T., HOUSTON, J.B. & HUANG, S.M. (2001). Optimizing drug development: strategies to assess drug metabolism/transporter interaction potential – toward a consensus. *Pharm. Res.,* **18,** 1071–1080.

WILLIAMS, D.L.H. (1988). *Nitrosation*. New York: Cambridge University Press.

(Received July 11, 2005
Revised August 31, 2005
Accepted December 7, 2005
Published online 23 January 2006)